Clinically compatible instrumentation for accurate detection of fluorescence intensity and lifetime in turbid media

Ching-Wei Chang[a], William Lloyd[a], Robert Wilson[b], Gregory D. Gillispie[c] Mary-Ann Mycek[a,b]

[a]Department of Biomedical Engineering, University of Michigan, Ann Arbor, MI, USA
[b]Applied Physics Program, University of Michigan, Ann Arbor, MI, USA
[c]Fluorescence Innovations, Bozeman, MT, USA

ABSTRACT

We report data collected with a specialized transient digitizer, high repetition rate microchip laser sources, and fiber optic light delivery and collection for rapid remote sensing in tissue-simulating phantoms. The instrumentation is highly suitable for eventual translation to a clinical setting owing to the speed of data acquisition and small footprint. Ranges for data acquisition time and instrument sensitivity were determined by measuring wavelength time matrices (WTMs) from tissue-simulating phantoms. Accuracy of WTM data was validated by comparison with Monte-Carlo simulations of fluorescent light propagation in turbid media.

Keywords: fluorescence spectroscopy, fluorescence lifetime, turbid media, photon propagation in tissue, tissue phantoms

1. INTRODUCTION

Fluorescence sensing shows promise for a wide variety of applications in tissue diagnostics because it is quantitative, non-invasive, objective, and non-destructive [1]. Fluorescence wavelength-time matrices (WTMs) are composed of fluorescence decay curves collected for a range of user-specified emission wavelengths. The information-rich nature of WTM data shows promise for a wide-range of biomedical optics applications, including tissue engineering applications. The specialized transient digitizer shows promise for improving the current gold standard of histology. Histology is invasive, qualitative, and subjective. In this study we report novel, clinically translatable instrumentation for the accurate detection of fluorescence intensity and lifetime in tissue-simulating phantoms. Experiments were performed on tissue-simulating phantoms composed of polystyrene microspheres embedded in either a gelatin matrix or collagen gel matrix. Monte-Carlo simulations [2, 3] were employed to determine the accuracy of the instrumentation and phantoms.

2. METHODS

2.1 Novel instrumentation for wavelength-time matrix measurements

Fig. 1 shows the instrumentation lay-out used when conducting experiments on tissue-simulating phantoms to collects WTMs. It consists of a 473 nm microchip laser (3 kHz pulse repetition, 1-3 ns pulse width) coupled into 600 μm diameter fiber optic probes for remote sensing of florescence in tissue simulating phantoms. A specialized transient digitizer (Fluorescence Innovations, Inc.) is used for fluorescence WTM detection. The detection fiber-optic probe is mounted to a micrometer stage whereas the excitation probe is fixed in position, allowing for detection probe movement in the horizontal direction and enabling variable center-center source-detector spacing.

Advanced Biomedical and Clinical Diagnostic Systems VIII, edited by Tuan Vo-Dinh, Warren S. Grundfest, Anita Mahadevan-Jansen, Proc. of SPIE Vol. 7555, 755503 · © 2010 SPIE · CCC code: 1605-7422/10/$18
doi: 10.1117/12.845789

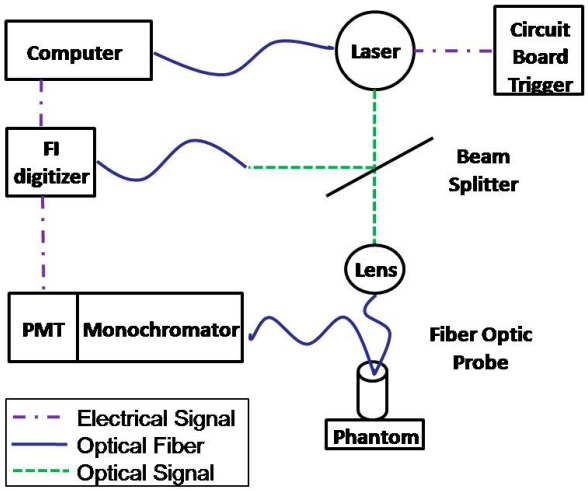

Figure 1. Instrumentation lay-out developed to collect WTMs from tissue-simulating phantoms.

2.2 Fluorescence wavelength-time matrices (WTMs)

WTMs of fluorescent intensity temporal decay at different wavelengths (illustrated in Fig. 2) [4-6] can be measured using the specialized digitizer described previously. Two dimensions of fluorescence information are within a WTM: wavelength-resolved and time-resolved. Integrating the WTM measurements over wavelengths yields the fluorescence temporal decay traditionally measured in time-resolved fluorescence lifetime spectroscopy experiments. Similarly, integrating the WTM over time yields the fluorescence spectrum traditionally measured in fluorescence spectroscopy experiments.

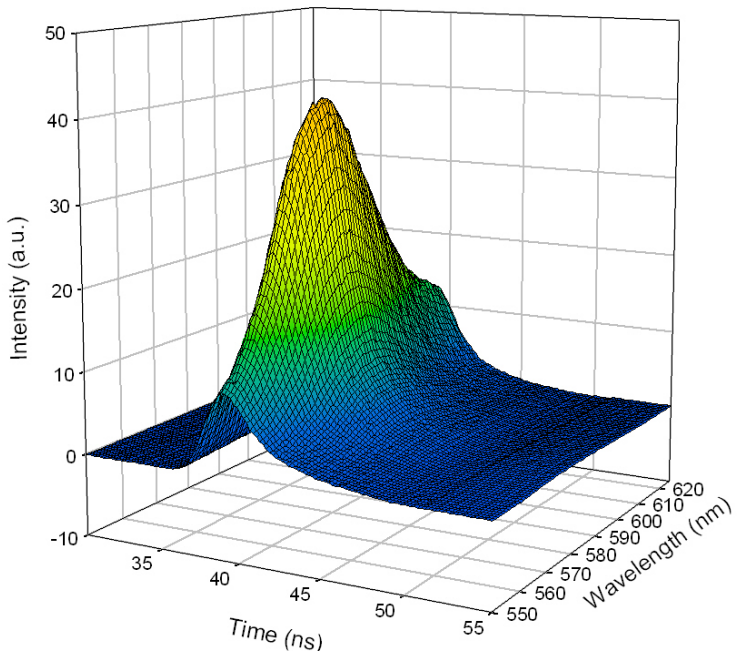

Figure 2. WTM of 1μM Rhodamine B in water: fluorescence intensity was recorded as a function of both wavelength of emission and the time following sample excitation.

Fluorescence lifetimes can be extracted from the temporal data of the WTM by implementing a least-squares fitting algorithm and a corresponding instrument response. Similarly, global fitting can be employed on WTMs acquired to extract the number of components and the lifetime of each component when the sample is composed of multiple fluorophores.

2.3 Tissue phantom preparation

Tissue phantoms consisting of fluorescent beads embedded in gel were developed to mimic tissue engineered constructs under study in our laboratory. The first set of phantoms was constructed with fluorescent beads (A7303, Invitrogen) and gelatin. One packet of gelatin powers (~7 g) were first dissolved in 240 ml boiled water, and then 120 ml of cold water was added to the solution. 896.6 µl of this solution was then mixed with 175.3 µl bead solution to achieve a final solution with concentration of gelatin ~15 mg/ml and concentration of beads = 1.67×10^5 beads per 60 µl gel. This mixture was poured into one 35 mm Petri dish, and then incubated at 4^O C overnight for solidification.

The second set of phantoms consisted of rat-tail collagen (#354236, BD Biosciences; 3.68 mg/ml) and the fluorescent beads mentioned above. The materials were first kept cold on ice and then mixed in an ice-cold tube in the following order: 100 µl ice cold 10X PBS, 27.7 µl ice cold 1N NaOH, 175.3 µl bead solution, and then 769 µl collagen solution. Air bubbles were avoided during mixing. The mixture was transferred to a 35 mm Petri dish, and then the dish was put in an incubator at 37^O C for half hour to solidify. The final gel mixture had the following concentrations: 2.64 mg/ml collagen and 1.67×10^5 beads per 60 µl gel.

2.4 Experimental Methods

Temporal range for WTM acquisitions are fixed from 0 – 127.8 ns with a time resolution of 0.2 ns. Wavelength parameters for WTM collections are specified prior to the start of the experiment by defining a start and end wavelength, as well as selecting the wavelength resolution (≥ 0.01 nm). For this study, each phantom was measured from 535-700 nm, resolution of 1 nm. WTMs were collected from each phantom described previously. Backgrounds were taken with gelatin and collagen samples of the same thickness in order to allow for spectra correction. Separate trials of 0 mm probe spacing and with 1.25 mm probe separation to analyze the effects of tissue parameters with variable probe spacing.

2.5 Monte-Carlo (MC) simulations

Monte Carlo (MC) models of time- and wavelength-resolved fluorescence [7] were employed for comparison with experimentally measured data in order to validate the accuracy of the instrumentation and phantoms. In the MC simulations, the collagen and beads sample was approximated as a homogeneous slab with reduced scattering coefficient μ_s' of 1 cm^{-1} and thickness of 4 mm. The value of μ_s' was estimated from measurements of diffuse reflectance and transmittance with an integrating sphere [7]. However, since we did not perform a collimated transmittance measurement to separate μ_s' into the scattering coefficient μ_s and the anisotropy g, we set g equal to 0.9 (a commonly-used approximation for biological tissue). Therefore, using the equation $\mu_s' = \mu_s (1 - g)$, the scattering coefficient in the simulations was $\mu_s = 10$ cm^{-1}. Simulations were run with three different values for the mean fluorescence lifetime: $\langle \tau \rangle$ = 1 ns, 2 ns, and 3 ns. The MC code was also employed to generate a wavelength-resolved fluorescence spectrum for the sample of collagen and fluorescent beads that was interrogated by the non-spaced fiber probe configuration. To generate this spectrum, a set of 10 MC simulations were run for fluorescence quantum yield values ranging from 0.1 to 1.0 (in steps of 0.1), and for each simulation, the total detected fluorescence was recorded. A previously-measured fluorescence emission spectrum from the beads was used to map each input quantum yield value onto a specific emission wavelength (or pair of emission wavelengths). Under the assumption that the collagen in the sample did not contribute appreciably to the measured fluorescence in this wavelength range, the aforementioned method produced a simulated wavelength-resolved fluorescence emission spectrum from the tissue model of collagen and beads at wavelengths of 530 nm to 643 nm.

3. RESULTS

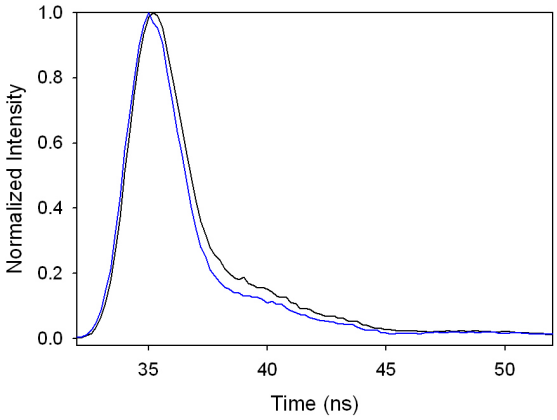

Figure 3. Comparison of normalized decay curves at 550 nm of beads in a gelatin matrix with different bead concentrations: The concentration described in secion 2.3 (1 x bead in blue) and the doubled concentration (2 x bead in black).

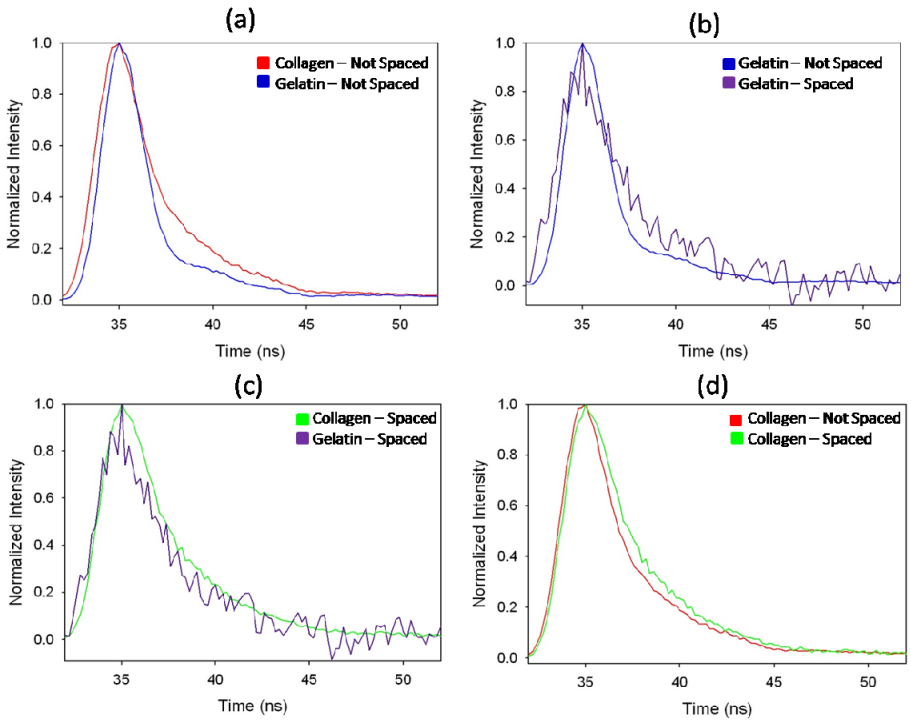

Figure 4. Comparison of decay curves at 550 nm of fluorescent beads in a gelatin matrix or collagen matrix with either no probe spacing or that of 1.25 mm. (a) Phantoms with no probe spacing were compared for collagen (red) phantom to gelatin (blue) phantom. (b) Probe spacing effects were analyzed by plotting gelatin with no spacing (blue) versus gelatin with 1.25 mm spacing (purple). (c) 1.25 mm probe spacing for gelatin phantom (purple) and collagen phantom (green). (d) Variable probe spacing for collagen phantom for no probe spacing (red) and 1.25 mm probe spacing (green). It can be observed that several factors affected the decay time of the fluorescence from the phantoms. (a) shows that fluorescence from collagen phatoms had an extended decay time as compared to gelatin phantoms as well as introducing a 1.25 mm separation between probes (b,d). (c) compares 1.25 mm probe spacing for collagen and gelatin phantoms, showing the same trend as (a) that fluorescence from gelatin phatoms had a shorter decay time than that from collagen phantoms.

The time-resolved fluorescence decay curves in Fig. 3 and Fig. 4 were collected using 1250 shots averaged per decay curve. For these experiments, wavelength-resolved spectra were collected from 535 nm to 700 nm. To collect a WTM for this range, acquisition time is ~1.15 minutes. Acquisition time can be shortened by decreasing the number of wavelengths collected (increase spacing or decrease spectral window) or by reducing the number of shots averaged if high signal-to-noise is still maintained.

Figure 3 demonstrates that when the concentration of the fluorescent beads was increased in the gelatin-based phantom sample, the fluorescence decay from the beads was prolonged. The effect of doubling the concentration of beads was to change the scattering properties of the phantom, and thus the fluorescence propagation in the tissue to detection probe.

We consistently observed a prolonged fluorescence decay curve in the collagen samples compared to that in the gelatin samples (Fig. 4 (a) and Fig. 4 (c)) in both spacing distances. In addition, fluorescence decay curve acquired with 1.25 mm spacing was also consistently prolonged compared to that acquired with no spacing between the excitaiton and detection probes (Fig. 4 (b) and Fig. 4 (d)) in both gelatin- and collagen-based samples. This was very likely, again, due to different degrees of photon scattering in the phatoms. With a longer photon traveling path when using 1.25 mm spacing, photons were subjected to more scattering events before being detected. As for the scattering property of collagen compared to gelatin, although in our phantoms the concentration of gelatin was higher, we indeed expected more scattering from collagen molecules due to their more anisotropic and organized structures. Since gelatin molecules are generally denatured and hydrolized collagen, much less scattering should be expected.

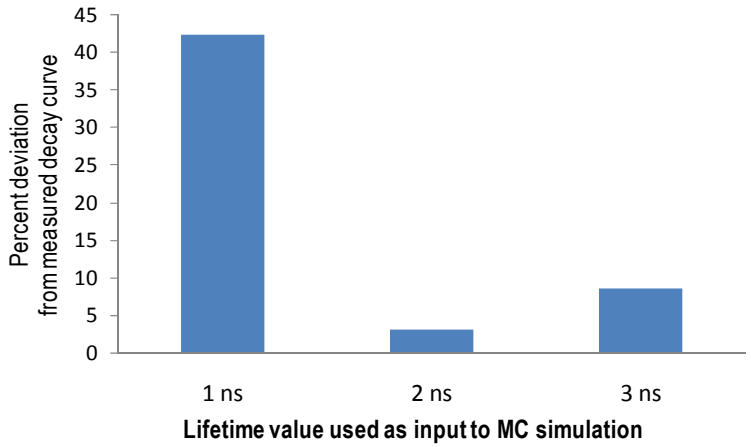

Figure 5. Percent deviations (calculated from 1-2.5 ns) between measured fluorescence decay curve and decay curves obtained from three MC simulations with mean lifetime values of 1 ns, 2 ns, and 3 ns used as inputs parameters.

A fluorescence lifetime value was extracted for the WTM from the collagen phantom with no probe spacing at 550 nm by using a least-squares fitting algorithm and the corresponding instrument response from a reflecting background. The extracted lifetime of 2.18 ns was shown to have less than 4% deviation from the simulated decay curves with input lifetime of 2 ns (Fig. 5, middle bar).

The experimentally measured wavelength-resolved fluorecence spectrum from the sample of collagen and beads, measured with the non-spaced probe, was compared to the simulated wavelength-resolved fluorescence spectrum. The simulated wavelength-resolved spectrum from 543 nm to 643 nm was shown to agree with the experimental measurement to better than 14%. One possible source of error is that the simulations did not account for the fact that the measured reduced scattering coefficient varied slightly as a function of wavelength.

4. CONCLUSIONS AND DISCUSSION

In this study, the effects of altering excitation-detection probe spacing, concentration of fluorescent beads, and phantoms made in a gelatin or collagen matrix were analyzed. It was shown that collagen phantoms have a prolonged decay due to the increased scattering parameters as compared to the gelatin matrix. This trend was seen in phantoms with no probe

spacing and with 1.25 mm probe spacing. Likewise, it was shown that the probe spacing in a given phantom will extend the decay as compared to the decay measured with no probe spacing.

The instrumentation reported here is also highly suitable for eventual translation to a clinical biomedical setting due to its accuracy, speed of data acquisition, portability, and the information-rich nature of the WTM fluorescence data. Promise is shown for application of this instrumentation in a variety of biomedical optics applications.

ACKNOWLEDGEMENTS

This work was supported in part by National Institutes of Health grants R43-EB-007866 (to G.D.G. and M.-A.M.) and R01-CA-114542 (to M.-A.M.).

REFERENCES

[1] M. A. Mycek and B. W. Pogue, Eds, Handbook of Biomedical Fluorescence, Marcel-Dekker Inc., New York, New York (2003).

[2] K. Vishwanath, B. Pogue and M. A. Mycek, "Quantitative fluorescence lifetime spectroscopy in turbid media: comparison of theoretical, experimental and computational methods," Physics in Medicine and Biology 47(18), 3387-3405 (2002)

[3] K. Vishwanath and M. A. Mycek, "Time-resolved photon migration in bi-layered tissue models," Optics Express 13(19), 7466-7482 (2005)

[4] A. J. Bystol, T. Thorstenson and A. D. Campiglia, "Laser-induced multidimensional fluorescence spectroscopy in Shpol'skii matrixes for the analysis of polycyclic aromatic hydrocarbons in HPLC fractions and complex environmental extracts," Environmental Science & Technology 36(20), 4424-4429 (2002)

[5] A. J. Bystol, A. D. Campiglia and G. D. Gillispie, "Laser-induced multidimensional fluorescence spectroscopy in Shpol'skii matrixes with a fiber-optic probe at liquid helium temperature," Analytical Chemistry 73(23), 5762-5770 (2001)

[6] A. J. Bystol, A. D. Campiglia and G. D. Gillispie, "Time-resolved laser-excited Shpol'skii spectrometry with a fiber-optic probe and ICCD camera," Applied Spectroscopy 54(6), 910-917 (2000)

[7] M. Chandra, K. Vishwanath, G. D. Fichter, E. Liao, S. J. Hollister and M. A. Mycek, "Quantitative molecular sensing in biological tissues: an approach to non-invasive optical characterization," Optics Express 14(13), 6157-6171 (2006)